Journal of Cell Science 111, 2855-2866 (1998)
Printed in Great Britain © The Company of Biologists Limited 1998
JCS4495

Localisation of Nramp1 in macrophages: modulation with activation and infection

Susan Searle[1,*], Nicholas A. Bright[2], Tamara I. A. Roach[3], Peter G. P. Atkinson[4], C. Howard Barton[4], Robert H. Meloen[5] and Jenefer M. Blackwell[1]

[1]Department of Medicine, University of Cambridge Clinical School, Level 5, Addenbrooke's Hospital, Hills Road, Cambridge CB2 2QQ, UK
[2]Department of Clinical Biochemistry, University of Cambridge Clinical School, Level 4, Addenbrooke's Hospital, Hills Road, Cambridge CB2 2QQ, UK
[3]Department of Infectious Diseases, University of Washington School of Medicine, St Louis, Missouri, USA
[4]University of Southampton, Biochemistry and Molecular Biology Research Division, School of Biological Sciences, Bassett Crescent East, Southampton SO16 7PX, UK
[5]Molecular Recognition, ID-DLO, Research Head Office, Edelhertweg 15, P.O. Box 65, 8200 AB Lelystad, The Netherlands
*Author for correspondence (e-mail: SS10057@MEDSCHL.cam.ac.uk)

Accepted 27 July; published on WWW 9 September 1998

SUMMARY

The murine natural resistance-associated macrophage protein, Nramp1, has multiple pleiotropic effects on macrophage activation and regulates survival of intracellular pathogens including *Leishmania, Salmonella* and *Mycobacterium* species. Nramp1 acts as an iron transporter, but precisely how this relates to macrophage activation and/or pathogen survival remains unclear. To gain insight into function, anti-Nramp1 monoclonal and polyclonal antibodies are used here to localise Nramp1 following activation and infection. Confocal microscope analysis in uninfected macrophages demonstrates that both the mutant (infection-susceptible) and wild-type (infection-resistant) forms of the protein localise to the membranes of intracellular vesicular compartments. Gold labelling and electron microscopy defines these compartments more precisely as electron-lucent late endosomal and electron-dense lysosomal compartments, with Nramp1 colocalizing with Lamp1 and cathepsins D and L in both compartments, with macrosialin in late endosomes, and with BSA-5 nm gold in pre-loaded lysosomes. Nramp1 is upregulated with interferon-γ and lipopolysaccaride treatment, coinciding with an increase in labelling in lysosomes relative to late endosomes and apparent dispersion of Nramp1-positive vesicles from a perinuclear location towards the periphery of the cytoplasm along the microtubular network. In both control and activated macrophages, expression of the protein is 3- to 4-fold higher in wild-type compared to mutant macrophages. In *Leishmania major*-infected macrophages, Nramp1 is observed in the membrane of the pathogen-containing phagosomes, which retain a perinuclear localization in resting macrophages. In *Mycobacterium avium*-infected resting and activated macrophages, Nramp1-positive vesicles migrated to converge, but not always fuse, with pathogen-containing phagosomes. The Nramp1 protein is thus located where it can have a direct influence on phagosome fusion and the microenvironment of the pathogen, as well as in the more general regulation of endosomal/lysosomal function in macrophages.

Key words: Nramp1, Late endosome, Lysosome, Phagosome

INTRODUCTION

The *Lsh/Ity/Bcg* gene was identified in mice for its role in regulating resistance and susceptibility to intracellular pathogens: *Leishmania donovani*, *Salmonella typhimurium*, *Mycobacterium bovis* and *M. intracellulare* (reviewed by Blackwell, 1989; Schurr et al., 1991). It is also a major candidate gene for autoimmune disease susceptibility in man (reviewed by Blackwell and Searle, 1998). A candidate for *Lsh/Ity/Bcg*, *Nramp1* (natural resistance-associated macrophage protein), was identified by positional cloning (Vidal et al., 1993) and the full-length sequence obtained (Barton et al., 1994), and its candidacy was confirmed using transfected macrophages in vitro (Barton et al., 1995) and gene disruption in vivo (Vidal et al., 1995). Murine *Nramp1* expression is macrophage-restricted and affects the capacity of the host to control intracellular replication of micro-organisms, all of which ultimately reside in the phagolysosome. Susceptibility is associated with a non-conservative amino acid substitution at position 169 (glycine^{resistant} to aspartic acid^{susceptible}), caused by a point mutation in the region encoding the fourth putative transmembrane spanning domain (TMD; Vidal et al., 1995). The polypeptide Nramp1 is a hydrophobic integral membrane protein, with the following predicted features: 10-12 TMDs, a

glycosylated extracellular loop and several phosphorylation sites (Vidal et al., 1993; Cellier et al., 1995, 1996); an amino-terminal putative SH3 binding domain (Barton et al., 1994); and structural features characteristic of prokaryote and eukaryote transporters and ion channels (Cellier et al., 1996). The yeast homologue, SMF1, functions as a Mn^{2+} transporter (Supek et al., 1996). Mammalian Nramp2 functions as a broad specificity metal iron transporter, transporting Fe^{2+}, Zn^{2+}, Mn^{2+}, Co^{2+}, Cd^{2+}, Cu^{2+}, Ni^{2+} and Pb^{2+} (Gunshin et al., 1997). The same study reported that Nramp1 transfection into *Xenopus* oocytes mediates enhanced uptake of Fe^{2+}. Other studies support the observation that Nramp1 regulates, and is regulated by, cellular iron levels: (1) Atkinson et al. (1997) demonstrated that chelation of iron with deferoxamine influences Nramp1 protein expression in interferon-γ and lipopolysaccharide (LPS)-activated macrophages; and (2) Atkinson and Barton (1998) show that ectopic expression of Nramp1 in COS-1 cells modulates iron accumulation. Precisely how its function as an iron transporter relates to the multiple pleiotropic effects of Nramp1 on macrophage activation and pathogen survival is unclear (reviewed by Blackwell and Searle, 1998), but a clear understanding of its localisation during activation and infection is crucial to defining function.

Initial studies using confocal microscopy localised the Nramp1 protein to the membranes of cytoplasmic vesicles in resting and activated bone marrow-derived macrophages (Atkinson et al., 1997), with evidence of colocalisation to late endosomal and lysosomal compartments in resident peritoneal macrophages (Gruenheid et al., 1997). Atkinson et al. (1997) identified the protein on vesicles in both wild-type (infection-resistant) and mutant (infection-susceptible) macrophages, but Gruenheid et al. (1997) did not detect protein expression in Nramp1 mutant macrophages. Both studies demonstrated that Nramp1 was recruited to the membrane of IgG bead (Atkinson et al., 1997) or latex bead (Gruenheid et al., 1997) phagosomes, but pathogen-induced phagosomes were not examined. This is important since, although phagocytosis of *Leishmania*, *Salmonella* and *Mycobacteria* results in internalisation and formation of a phagosome from the plasma membrane, the subsequent fate of this newly formed organelle differs with the different pathogens. *Leishmania* spp. (e.g. Lang et al., 1994) and *S. typhimurium* (Rathman et al., 1996, 1997) phagosomes undergo rapid fusion with acidic compartments to produce mature phagolysosomes. In *M. avium*- and *M. tuberculosis*-infected macrophages, maturation of the phagosome is arrested in an early transitional stage, which prevents or delays the formation of a mature phagolysosome (Sturgill-Koszycki et al., 1994, 1996). A more detailed analysis of the localisation of the protein during activation and infection would assist in defining Nramp1 function in relation to these two important processes. Here we present new data on the localisation of Nramp1 following activation of macrophages and during infection with leishmanial and mycobacterial pathogens.

MATERIALS AND METHODS

Production of polyclonal and monoclonal anti-Nramp1 antibodies

Polyclonal antibody against the C-terminal 35 amino acids of the Nramp1 antibody was prepared and affinity-purified as previously described (Atkinson et al., 1997). Polyclonal rabbit and monoclonal rat anti-mouse N-terminal Nramp1 antibodies were raised against Nramp1-pGEX1 (Smith and Johnson, 1988) fusion proteins prepared with nucleotides encoding amino acids 2-82 of *Nramp1* in-frame with the glutathione-S-transferase gene. Fusion proteins were mixed with Ribi adjuvant (Ribi ImmunoChem Research, Inc. Hamilton, Mt US) and inoculated into rats using a combination of subcutaneous, intraperitoneal and intravenous immunisations as described (Clark and Waldmann, 1986). Hybridomas were produced using standard polyethylene glycol (Boehringer-Mannheim UK Ltd, Lewes, England) fusion of splenic B cells to the Y3-Ag1.2.3 myeloma line, followed by hypoxanthine, aminopterin and thymidine (HAT; Gibco-BRL, Paisley, UK) as described (Clark and Waldmann, 1986). Screens were performed by ELISA using total cell lysate obtained by sonication of activated (1 ng/ml LPS, Sigma Chemical Co. Ltd, Poole, UK; 25 units/ml murine recombinant interferon-γ, Genzyme Diagnostics, West Malling, England) resident peritoneal macrophages from congenic B10.L-*Lsh*^{r} (Nramp1 wild type) mice (Blackwell et al., 1988). Second layer detection was with biotinylated rabbit anti-rat IgG (heavy plus light chain; mouse adsorbed; affinity-purified; 1:300), followed by streptavidin peroxidase (Dako Ltd, High Wycombe, England).

Macrophage populations

Monoclonal hybridoma supernatants were screened by confocal microscopy using a range of macrophage cell types: (1) the *Nramp1* mutant BALB/c mouse-derived RAW264.7 macrophage cell line (Raschke et al., 1978), and RAW264.7 clones stably transfected with mutant (2S and 10S) or wild-type (7.5R) *Nramp1* expressed under a viral LTR promoter (Barton et al., 1995); (2) the *Nramp1* wild-type DBA/2 mouse-derived P388D1 macrophage cell line (Dawe and Potter, 1957); (3) resident peritoneal macrophages from C57Bl/10ScSn (*Nramp1* mutant) or congenic N20 B10.L-*Lsh*^{r} (*Nramp1* wild type) mice; (4) 10-day bone marrow-derived macrophages from C57BL/10ScSn or congenic N20 B10.L-*Lsh*^{r} mice prepared as described (Roach et al., 1993) using L-cell-conditioned medium. All macrophage populations were examined with/without 24 hours activation with 25 ng/ml LPS and 25 units/ml interferon-γ. Primary bone marrow-derived macrophages from congenic *Nramp1* wild-type and mutant mice were also used for electron microscope gold-labelling (EM-gold) localisation studies. Macrophages were grown on bacterial grade plates, with/without 100 units/ml recombinant interferon-γ and 50 ng/ml LPS, for 24 hours prior to preparation of cell pellets for EM.

Macrophage infections

Macrophages were infected with a 10:1 pathogen:macrophage ratio. RAW264.7 2S, 10S or 7.5R stable transfectants were infected with *L. major* LV39 metacyclics for 24 hours as described (Cooper et al., 1988). Infection of primary bone marrow-derived macrophages with *M. avium* 101 (gift from Prof. David Russell, Washington University, School of Medicine) was carried out as described (Schaible et al., 1998). Briefly, 10-day macrophage cultures were transferred to glass slides 3 days prior to infection, and infected in antibiotic-free medium supplemented with 5% horse serum for 2 hours at 37°C. The cells were washed to remove external bacteria and cultured for a further 2 hours prior to fixation. Macrophages were activated with interferon-γ (400 units/ml) for 16 hours and LPS (500 ng/ml) for 4 hours prior to infection.

Epitope mapping of anti-Nramp1 monoclonal antibodies

Attempts to western blot with mAbs were unsuccessful. To ensure that antibodies were reactive with the N terminus of Nramp1, epitope mapping was performed using overlapping peptides synthesised in credit-card format on miniPEPSCAN cards as described (Slootstra et al., 1996). The binding of mAbs was tested in an ELISA and quantified by a CCD camera and image processing system.

Immunostaining and confocal microscopy

Immunostaining for confocal microscopy was performed as described (Atkinson et al., 1997) for rabbit antisera. A similar protocol for rat mAbs was used except that cells were pre-incubated with 10% normal rabbit serum (DAKO Ltd., High Wycombe, England) and second layer detection was with biotinylated rabbit anti-rat IgG (1:300; B1022, Vector Laboratories Inc., Peterborough, UK). Nuclei were visualised by counterstaining with propidium iodide (5 ng/ml; Sigma Chemical Co. Ltd, Poole, UK). For double staining with endocytic markers (see antibody reagents), incubations with primary antibodies were performed sequentially with pre-incubation in 10% normal horse serum or normal swine serum, and second layer detections using a horse anti-mouse IgG Texas Red direct conjugate that cross-reacts with rat IgG (1:400; Vector Laboratories Inc.) or biotinylated swine anti-rabbit IgG (1:300; DAKO) and streptavidin FITC (1:100; DAKO), as appropriate. Cells were viewed with a Nikon optiphot-2 epifluorescence microscope coupled to a Bio-Rad MRC1000 confocal laser scanning attachment (Bio-Rad, Hemel Hempstead, UK). The microscope settings were standardised within experiments, as indicated in the figure legends.

Antibody reagents

For labelling of endocytic compartments, a range of antibodies were obtained. Rabbit IgG specific to rat cathepsins D and L, which cross-reacts with mouse proteins (Wiederanders and Kirschkle, 1986), and rat anti-mouse macrosialin IgG2a (Smith and Koch, 1987) were kindly provided by Dr Thierry Lang (Institut Pasteur, Paris). A hybridoma cell line producing the mAb ID4B, which recognises mouse lysosomal associated protein Lamp1, was obtained from Prof. David Russell (Washington University, School of Medicine). Protein A conjugated to 10 nm or 15 nm colloidal gold (PAG) was from Department of Cell Biology, University of Utrecht. Goat anti-rat IgG conjugated to 10 nm gold particles and goat anti-rabbit IgG conjugated to 15 nm gold particles were from Agar Scientific Ltd (Stansted, UK).

Immuno-electron microscopy

Immuno-EM was performed on ultrathin frozen sections of bone marrow-derived macrophages prepared as described (Griffiths, 1993; Bright et al., 1997). Briefly, cells were washed in PBS and fixed in 8% paraformaldehyde/250 mM Hepes, pH 7.2, for 1 hour at room temperature prior to embedding in gelatin and infusion with sucrose. Sections were cut using a diamond knife mounted on a Reichert Ultracut S ultramicrotome with a cryochamber attachment (Leica, Milton Keynes, UK) and observed on a Philips CM 100 transmission electron microscope (Philips Electron Optics, Cambridge, UK) at an operating voltage of 80 kV.

Immunolabelling

Ultrathin cryosections of cells were indirectly single- or double-labelled using techniques described (Slot and Gueze, 1983; Slot et al., 1991). All antibodies and PAG conjugates were diluted in 1% BSA/PBS. Immunolabelling was performed as described (Bright et al., 1997). The grids were incubated with primary antibody for 1 hour at room temperature. Monocloncal anti-N-terminal Nramp1 antibodies were used as neat culture supernatant. Polyclonal anti-C-terminal Nramp1 was diluted 1:100. Rabbit antibodies were detected with PAG or goat anti-rabbit IgG 15 nm gold conjugate and rat mAbs were detected using goat anti-rat IgG 10 nm gold conjugate. For double labelling of cathepsins D and L with monoclonal anti-Nramp1, cells were incubated with anti-Nramp1, rinsed and incubated with goat anti-rat IgG-10 nm gold, washed and gold-labelled complexes stabilised. The procedure was repeated with marker antibodies and goat anti-rabbit IgG-15 nm gold. Similarly, for double labelling of polyclonal anti-Nramp1 with cathepsins D and L, the above procedure was followed substituting PAG 15 nm for specific labelling of Nramp1 and PAG 10 nm to give specific labelling of endocytic markers. For double labelling of Lamp1 or macrosialin with polyclonal anti-Nramp1, goat anti-rabbit IgG-15 nm gold was used to label Nramp1 and goat anti-rat IgG-10 nm gold for endocytic markers. The cells were washed in water and stained with 1.8% methyl cellulose/0.3% uranyl acetate (Tokuyasu, 1978).

Labelling of macrophages with BSA-gold

To load lysosomes but not late endosomes, primary bone marrow-derived macrophages grown to confluence were incubated with BSA-5 nm gold for 4 hours at 37°C followed by a 20-hour chase in medium free of conjugate. BSA-5 nm gold was prepared using tannic acid in sodium citrate to reduce gold choloride as described (Slot and Geuze, 1985).

Quantitation of Nramp1 expression

Semi-quantitative analysis of Nramp1 expression in different cell types with/without activation was scored on a scale ±, +, ++, +++, indicating increasing strength of fluorescent signal, using anti-N-terminal anti-Nramp1 mAbs. Quantitative analysis of the subcellular distribution of Nramp1 was performed on randomly selected EM cryosections, which were scored for the number of Nramp1-specific gold particles on electron-lucent late endosomes and electron-dense lysosomes. Results were recorded as mean (± s.e.m. for triplicate scores from wild type versus mutant, and resting versus activated, bone marrow-derived macrophages. The number of gold particles localised to lysosomal compartments were also expressed as a percentage (mean ± s.e.m.) of Nramp1-specific gold label in late endosomes.

RESULTS

Confocal microscope analysis of Nramp1 expression in different macrophage populations

Table 1 provides a semi-quantitative analysis of Nramp1 expression detected by three different anti-N-terminal mAbs examined in different cell types. All mAbs were screened initially by ELISA on inteferon-γ/LPS-activated resident peritoneal macrophages for Nramp1 wild-type B10.L-*Lsh*^{r} mice, and all were positive by confocal microscopy on this population (data not shown). On the RAW264.7 macrophage line, which carries an endogenous copy of the mutant allele, all three mAbs showed negative or weak Nramp1 staining. Similar results were obtained with the affinity-purified polyclonal anti-C-terminal antibody (Fig. 1A), even with interferon-γ/LPS-activation (data not shown). However, bright Nramp1-specific fluorescence was observed in RAW264.7 cells stably transfected with mutant (Fig. 1B) or wild-type (data not shown) Nramp1 constitutively expressed under a viral LTR (Barton et al., 1995). In unstimulated transfected cells, the protein was localised in vesicular compartments clustered around the perinuclear region (Fig. 1B). Following activation, staining became dispersed on vesicles throughout the cytoplasm, following a pattern appearing to coincide with the microtubular network of the cell in mutant (Fig. 1C) and wild-type (not shown) macrophages. Using monoclonal anti-N-terminal antibodies 3N7C3 and 3N7A4 on control (data not shown) and activated (Fig. 1D,E) P388D1 cells, a clear picture of vesicular staining following the pattern of cytoplasmic spread of macrophages was observed. For EM-gold analysis, we preferred to use macrophage populations expressing natural endogenous copies of mutant or wild-type Nramp1, to

Table 1. Semi-quantitative analysis of Nramp1 expression levels in different cell types

	Mϕ cell lines				BM-derived Mϕ			
	MT*		WT‡		MT¶		WT§	
Antibody	CT	γ/L	CT	γ/L	CT	γ/L	CT	γ/L
3N7C3	+	±	+	++	+	++	++	++
3N7C2	±	±	±	+	±	++	++	+++
3N7A4	±	±	±	++	+	++	++	+++

MT*, mutant RAW264.7; WT‡, wild type P388D1; MT¶, mutant C57BL/10ScSn (*Lsh*^{s}); WT§, wild type B10.L-*Lsh*^{r}.

Cells were resting (controls) or activated with 25 units/ml interferon-γ and 25 ng/ml LPS for 24 hours prior to fixation and permeabilisation for immunofluorescence. The subcellular localisation of Nramp1 observed by confocal microscopy showed changes in the level of Nramp1. ±, +, ++, +++, correlate with the increased strength of the fluorescent signal observed. Nramp1-specific staining in most cell types show an increase in the level of expression following stimulation with interferon-γ/LPS. The highest level of Nramp1 expression observed was in B10.L-*Lsh*^{r} and the lowest in RAW264.7.

CT, Control; γ/L, Interferon-γ/LPS.

determine whether there were fine ultrastructural differences in trafficking of the protein to the correct subcellular compartment. As with earlier studies using polyclonal anti-C-terminal antibody (Atkinson et al., 1997), we found that anti-N-terminal mAbs (Table 1 and, for example, mAb 3N7C2 in Fig. 1F) lit up both mutant and wild-type macrophages, with enhanced staining after activation. This therefore seemed an appropriate cell population to use in further ultrastructural analysis.

Epitope mapping of monoclonal and polyclonal antibodies

The affinity-purified polyclonal anti-C-terminal Nramp1 antibody was known to recognise a 65 kDa interferon-γ-inducible protein in murine macrophages and the fusion protein on western blotting (Atkinson et al., 1997). To ensure that anti-N-terminal mAbs were recognising Nramp1, epitope mapping was undertaken using the pepscan card system (Slootstra et al., 1996). 3N7C2 showed peak activity for an epitope spanning

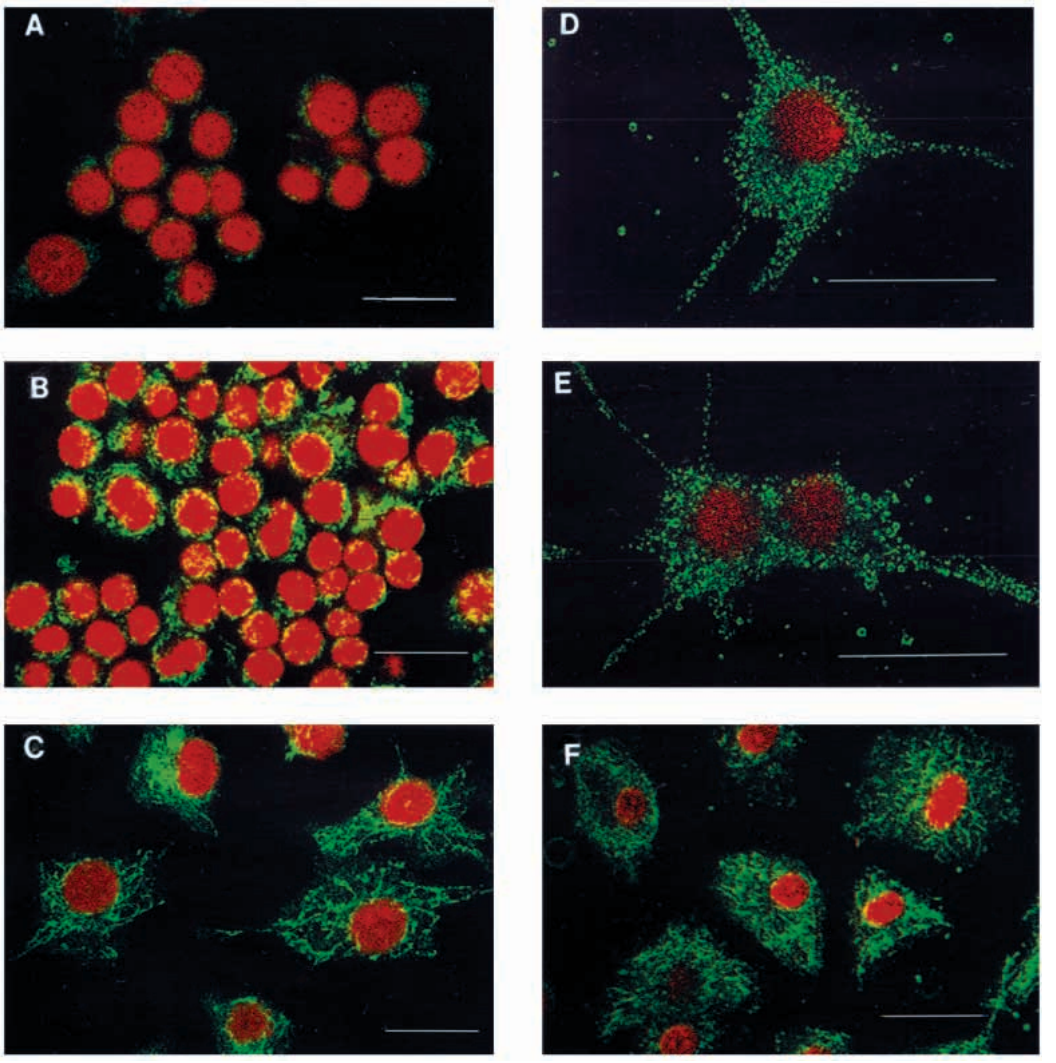

Fig. 1. Subcellular localisation of Nramp1 (green) in different macrophage populations. (A-C) Comparison of untransfected RAW264.7 cells (A) to resting (B) or interferon-γ/LPS-activated (C) Nramp1 mutant 10S stable transfectants. Cells were stained with affinity-purified rabbit anti-C-terminal Nramp1 polyclonal antibody. The mutant protein is clearly expressed in the 10S transfectant, and the distribution influenced by activation. Similar results were obtained with 7.5R Nramp1 wild-type transfectants. (D-F) Localisation of Nramp1 in interferon-γ/LPS macrophages using anti-N-terminal mAbs. P388D1 (Nramp1 wild type; D,E) and C57BL/10ScSn (Nramp1 mutant; F) macrophages labelled with mAbs 3N7C3 (D), 3N7A4 (E) or 3N7C2 (F). Nramp1 clearly localises to intravesicular compartments with a distribution pattern characteristic of late endosomes and lysosomes. Nuclei were stained with propidium iodide (red). Microscope settings: gain −1500; black level −2 (A-C) or −5 (D-F); iris 3 (A), 4 (B,C), 2.6 (D,E) or 3.5 (F) on the FITC channel. Bars, 25 μm.

Table 2. Epitope sequences recognised by Anti-Nramp1 mAbs

Peptide sequence – 3N7C2	A_{ccd}	Peptide sequence – 3N7C3	A_{ccd}
L R K L W A F T G P	794	A D Q G T F S L R K	439
R K L W A F T G P G	1006	D Q G T F S L R K L	542
K L W A **F T G P G F**	1986	Q G T F S **L R K L W**	773
L W A **F T G P G F** L	2406	G T F S **L R K L W** A	634
W A **F T G P G F** L M	1703	T F S **L R K L W** A F	906
A **F T G P G F** L M S	1596	F S **L R K L W** A F T	849
F T G P G F L M S I	1783	S **L R K L W** A F T G	634
T G P G F L M S I A	239	**L R K L W** A F T G P	602
G P G F L M S I A	619	R K L W A F T G P G	354
		K L W A F T G P G F	314

Nramp2
S F R K L W A F T G P G F L M S I A

Nramp2
E E Y S C F S F R K L W A F T G P G F

Peptide sequences of Nramp1 recognised by mAbs 3N7C2 and 3N7C3. Epitopes predicted by pepscan analysis of overlapping peptides (10 amino acids in length) spanning amino acids 2-82 in the N terminus of Nramp1 are in bold and underlined. The homologous sequence of Nramp2, spanning the Nramp1 peptide sequences, are shown. These adjacent epitopes lie within the predicted TMD1. A_{ccd} shows the fluorescence intensity above background.

amino acids FTGPGF at positions 58-63 of the N-terminal sequence, and 3N7C3 for amino acids LRKLW at positions 52-56 (Table 2). These epitopes map to a previously defined membrane-associated region, TMD1 (Cellier et al., 1995). Polyclonal anti-N-terminal Nramp1 mapped to an Nramp1-specific epitope spanning amino acids PSADQGFT at position 43-50. While the mAb epitopes are shared with Nramp2, northern analysis with Nramp2-specific probes reveals no expression of Nramp2 in resting or activated macrophage populations (C. H. Barton, unpublished observation). Monoclonal antibodies 2N7C3 and 3N7A4 (which shows very clear cellular localisation, Fig. 1E), could not be mapped. Hence 3N7C2, which showed strong reactivity with primary bone marrow-derived macrophages from both wild-type and mutant Nramp1 mice (Fig. 1F), was chosen for EM-gold analysis.

Immunogold-EM localisation of Nramp1 in resting versus activated bone marrow-derived macrophages

The organisation and morphology of the endosomal system in mouse peritoneal macrophages was previously defined utilizing a variety of antigenic markers in combination with endocytic tracers (Rabinowitz et al., 1992). Essentially the endosomal system in macrophages was found to be identical to compartments studied in non-phagocytic cells, i.e. four major compartments, early endosomes, multivesiclular bodies, late endosomes/prelysosomes and lysosomes. In this study macrophages were prepared in a similar manner and immunogold-EM localisation of Nramp1 performed on ultrathin cryosections. Anti-Nramp1 polyclonal and mAbs confirmed Nramp1 expression at the immunogold-EM level in bone marrow-derived macrophages from wild-type (Fig. 2A,B) and mutant (Fig. 2C) congenic mouse strains. Gold particles were localised to the membranes of electron-lucent (Fig. 2A,C) and electron-dense (Fig. 2B) organelles in both control (data not shown) and interferon-γ/LPS activated macrophages, with morphological characteristics of endosomes and lysosomes (Geuze et al., 1988; Griffiths et al., 1988; Mellman, 1996). This is consistent with the localisation of Nramp1 to intravesicular compartments demonstrated by confocal microscopy. Insufficient numbers of multivesicular bodies in our macrophage populations were observed to determine if they were Nramp1-positive. Cells stimulated with interferon-γ/LPS showed an increase in the frequency of labelled compartments with the anti-Nramp1 antibodies, indicative of increased protein expression as suggested by confocal analysis and previously shown by western blotting (Atkinson et al., 1997). In comparison to the wild-type protein, reduced labelling was observed in Nramp1 mutant macrophages. This was supported by quantitative analysis of the subcellular distribution of Nramp1 on late endosomes and lysosomes, which showed that wild-type macrophages (Fig. 3) consistently showed 3- to 4-fold more Nramp1-specific gold label than mutant macrophages on both late endosomes and lysosomes in both control and activated macrophages. Following activation, the majority of the label remained in the late endosomes, but there was an equivalent increase in the proportion of gold label in lysosomes relative to late endosomes in both wild-type and mutant macrophages (see inset, Fig. 3), coincident with the apparent dispersion of Nramp1-positive vesicles throughout the cells following activation (Fig. 1). This is consistent with previous studies showing that late endosomes are located in the perinuclear region of the cell whereas lysosomes are typically found throughout the cytoplasm (Geuze et al., 1988; Griffiths et al., 1988). In control experiments, anti-Nramp1 antibodies were omitted and no labelling with the gold conjugate was observed.

Colocalization of Nramp1 with late endosome/lysosome markers

To define and characterise these two morphologically distinct Nramp1-positive compartments more precisely, colocalization experiments were performed with antibodies against defined endocytic markers and either the anti-Nramp1 anti-C-terminal/N-terminal polyclonals or mAbs 3N7C2 and 2N7C3. This was accomplished initially by double-labelling experiments with antibodies directed against both late endosomal and lysosomal markers: Lamp1 (Geuze et al., 1988; Griffiths et al., 1988; Griffiths, 1993) and the lysosomal hydrolases cathepsins D and L (Wiederanders and Kirschke, 1986), which have previously been identified in endosomes (Geuze et al., 1985; Diment et al., 1988; Ludwig et al., 1991) and lysosomes (von Figura and Hasilik, 1986). Staining patterns of these markers were analysed by immunogold-EM

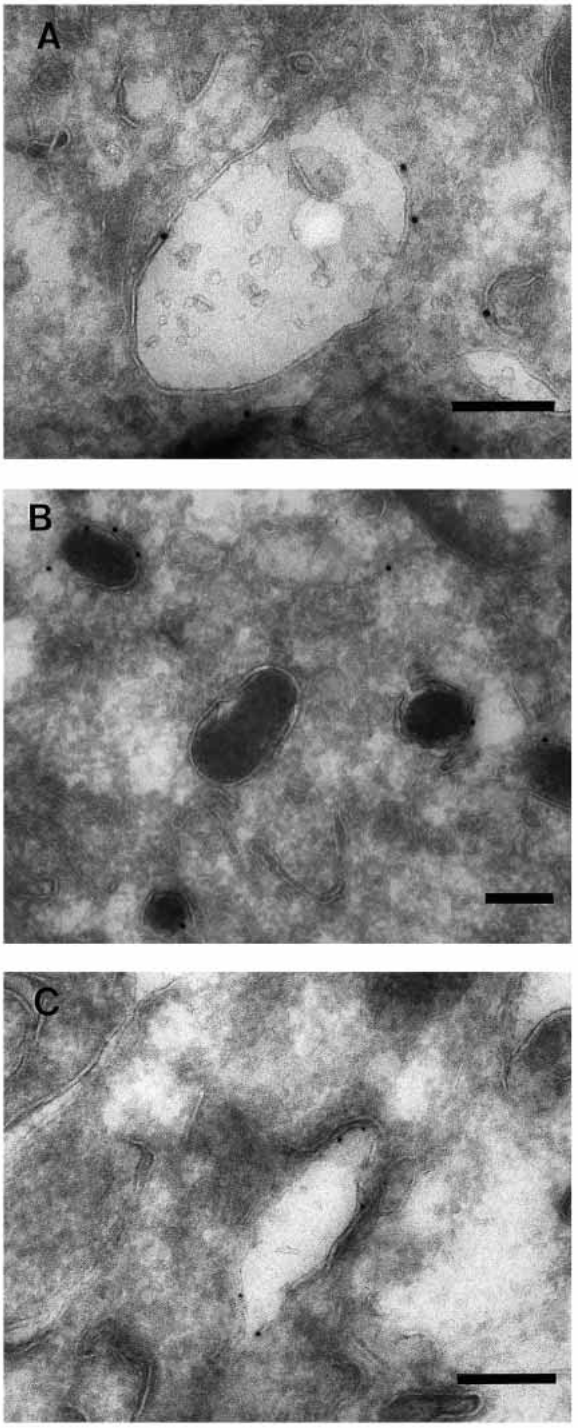

Fig. 2. EM micrographs of ultra-thin cryosections of activated bone marrow-derived macrophages from Nramp1 mutant C57BL/10ScSn versus congenic Nramp1 wild-type N20 B10.L-*Lsh*^{r} mice, labelled with anti-Nramp1 antibodies. Sections labelled with affinity-purified polyclonal anti-C-terminal Nramp1 or rat mAb 3N7C2 followed by PAG 15 nm or goat anti-rat IgG-10 nm gold, respectively. Wild-type (A,B) and mutant (C) macrophages were labelled with polyclonal anti-Nramp1 (A,B) or 3N7C2 (C). Polyclonal and monoclonal anti-Nramp1 antibodies label the membranes of endosomal/lysosomal organelles in Nramp1 mutant and wild-type macrophages. Similar results were obtained with mAb 3N7A4. Gold labelling was also observed in resting macrophages from both mouse strains, but at reduced levels. Bars, 200 nm.

on wild-type activated bone marrow-derived macrophages (Fig. 4) or by confocal microscopy on activated P388D1 macrophages (Fig. 5). Stimulation with cytokines increases both Nramp1 expression (this study and Govoni et al., 1995; Atkinson et al., 1997; Brown et al., 1997) and expression of lysosomal hydrolases (Lah et al., 1995). Here we observed that Lamp1 and Nramp1 colocalised to the membranes of late endosomes and lysosomes (Fig. 4A,B). Antibodies to cathepsin D decorated the membranes of late endosomes compatible with previous reports (Diment et al., 1988; reviewed by Authier et al., 1996), and the lumens of late endosomes and lysosomes in which membrane-localised Nramp1 labelling also occurred (Fig. 4C,D). Nramp1 was also observed to colocalise with cathepsin L in endosomal/lysosomal compartments (Fig. 5C). Similar results were observed at EM-gold level with the mAb 3N7C2 and cathepsins D and L (data not shown). To distinguish and further characterise Nramp1-labelled compartments, BSA-5 nm gold was allowed to accumulate predominantly in lysosomes and not late endosomes, following a 20-hour pulse chase experiment (Fig. 4E,F). Nramp1 is clearly present on organelles with late endosome morphology not loaded with gold (Fig. 4E) and on the membranes of BSA gold loaded lysosomes (Fig. 4F). Further confirmation of Nramp1's presence on late endosomes was demonstrated by confocal microscopy (Fig. 5F), where Nramp1 was observed to colocalise with macrosialin: a macrophage-specific membrane glycoprotein restricted to late endosomes and absent from lysosomes (Rabinowitz et al., 1992). Similar observations were made by EM-gold analysis (data not shown). Despite the lower overall anti-Nramp1 gold labelling of Nramp1 mutant bone marrow-derived macrophages, there were no qualitative differences in colocalization of the protein in subcellular compartments compared to wild-type macrophages (data not shown).

Localisation of Nramp1 in macrophages infected with intracellular pathogens

To gain insight into how Nramp1 might regulate survival of intracellular pathogens in macrophages, and to ascertain whether the mutated protein localises to the same compartments as wild type during infection, confocal microscopy of macrophages infected with *L. major* or *M. avium* was performed. Clear Nramp1-specific staining of *L. major* phagosomes in RAW264.7 2S (Fig. 6A), 10S or 7.5R (data not shown) stably transfected cells was observed. In these resting macrophages, the Nramp1-positive phagosomes are predominantly perinuclear in location, and the nuclei of the parasites are clearly visible within the Nramp1-positive vesicle, indicating that fusion between phagosomes and late endosomes/lysosomes has occurred. When Nramp1 wild-type bone marrow-derived macrophages were infected with *M. avium*, a more dramatic migration of Nramp1-positive vesicles (Fig. 6D) to the location of bacterial pathogens (compare with Fig. 6C) occurred within 2 hours in both resting (data not shown) and activated wild-type (Fig. 6C,D) macrophages. This contrasts with the dispersed pattern of Nramp1-positive vesicles seen in activated macrophages from Nramp1 wild-type mice (Fig. 6B). Many bacteria are seen directly within Nramp1-positive vesicles following infection of both resting and activated macrophages, but the rate of phagosome fusion to the late endosomal/lysosomal compartment could not be

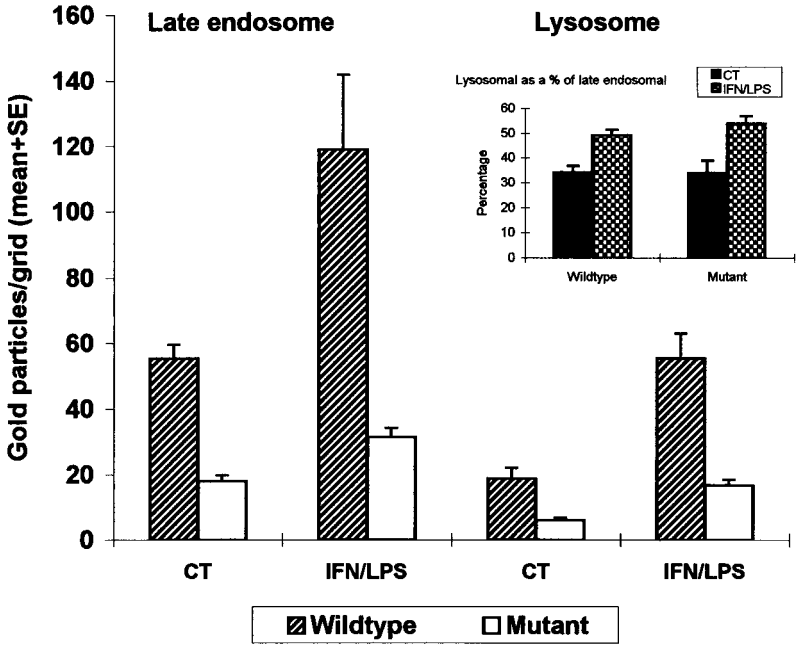

Fig. 3. Quantitative analysis of subcellular distribution of Nramp1 performed on randomly selected EM cryosections. Cryosections were scored for Nramp1-specific gold particles on electron-lucent late endosomes and electron-dense lysosomes. Results are shown as mean (± s.e.m. for triplicate scores from wild type versus mutant, and resting versus activated, bone marrow-derived macrophages. In the insert, the number of gold particles localised to lysosomal compartments are expressed as a percentage (mean ± s.e.m.) of Nramp1-specific gold label in late endosomes. CT, control; IFN/LPS, interferon-γ/LPS.

accurately quantitated. Interestingly, however, although migration of Nramp1-positive vesicles to the site of bacterial phagosomes was also observed in Nramp1 mutant-activated macrophages, this did not appear to occur as efficiently in infected resting mutant macrophages (Fig. 6E,F). This is consistent with previous EM studies showing reduced phagosome-lysosome fusion in macrophages from Nramp1 mutant BALB/c mice compared to their chromosome 1 congenic wild-type counterparts (de Chastellier et al., 1993). Hence, there may be qualitative and quantitative differences in the way Nramp1-positive vesicles are delivered to the pathogen-containing phagosome in leishmanial compared to mycobacterial infected cells, which could have important consequences for Nramp1-regulated antimicrobial activity. In both infection models, however, it is clear that interaction with the pathogen alone is sufficient to provide the stimulus for migration and/or fusion of Nramp1-positive vesicles with the infected phagosome.

DISCUSSION

Results presented here provide new data on epitope mapping of anti-N-terminal Nramp1 antibodies; on confocal and EM-gold localisation and quantitative expression of Nramp1 in late endosomal and lysosomal compartments of resting and activated Nramp1 wild-type and mutant macrophages; and on the localisation of Nramp1 in infected macrophages. Each of these findings sheds new light on Nramp1 function, and/or on areas of controversy in the Nramp1 literature.

Firstly, the fact that some of the anti-Nramp1 mAbs used in this study bind to epitopes in the first putative TMD suggests that previous structural predictions of 12 TMDs (Cellier et al., 1995, 1996) may be incorrect, since it is questionable that an immunogenic epitope would be positioned within a membrane. This has important implications for the function of the N terminus of the molecule, making the putative SH3 binding domain, which lies immediately 5′ of the first putative TMD, more accessible to protein-protein interactions in the cell which might regulate Nramp1 function.

A second area of interest in data presented here relates to the controversy surrounding production and localisation of the protein in macrophages bearing the mutant *Nramp1* allele. Vidal et al. (1996) and Gruenheid et al. (1997) failed to identify a protein in Nramp1 mutant macrophages either by immunoprecipitation or confocal microscopy. In contrast, Atkinson et al. (1997) identified a protein by western blotting and confocal microscopy. Although our observation that RAW264.7 macrophages were negative/weak for Nramp1 expression concurred with the former, we were able to demonstrate that expression of the Nramp1 mutant cDNA under a constitutive LTR promoter does lead to stable expression and localisation of the protein. We also found no defect in expression and EM-gold localization of the Nramp1 protein in Nramp1 mutant bone marrow-derived macrophages. This does not, however, preclude the possibility that differences in size and charge of the mutated amino acid may influence interactions with other amino acids that culminate in steric changes not observed by EM. This may affect maturation of the protein, an important pre-requisite for a functional membrane protein (High and Laird, 1997), or in some way alter the biochemical functions of Nramp1. Although there were quantitative differences in the level of Nramp1 expression induced during maturation of bone marrow-derived macrophages with L-cell conditioned medium, and following activation with interferon-γ/LPS, we chose this more uniformly induced pattern of endogenous Nramp1 expression in bone marrow-derived macrophages for more detailed ultrastructural studies of Nramp1 localisation.

Our third major contribution in relation to previous studies is to clarify the subcellular localisation of the Nramp1 protein. Fluorescence staining/confocal microscopy and EM-gold labelling performed with anti-Nramp1 polyclonal antibody and mAbs confirmed localisation of Nramp1 to the membranes of

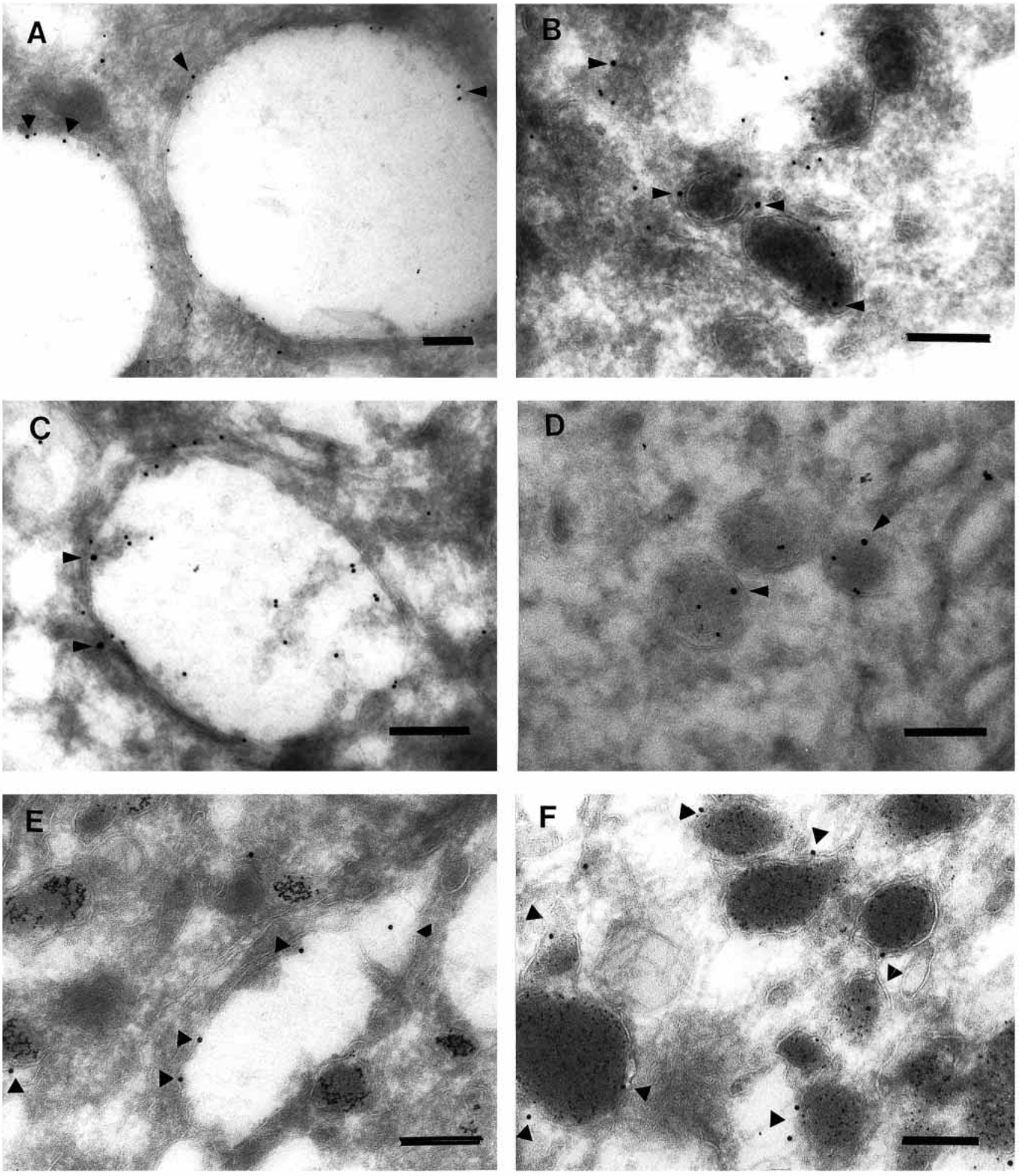

Fig. 4. Identification of the endocytic compartments to which Nramp1 localises. Ultrathin cryosections of activated bone marrow-derived macrophages double-labelled with affinity-purified polyclonal anti-C-terminal Nramp1 (15 nm gold; arrowheads) and endocytic markers (10 nm gold) Lamp1 or cathepsin D. (A,B) Colocalization of Nramp1 with Lamp1 to the membranes of late endosomal/lysosomal endocytic vesicles. (C,D) Examples of Nramp1 localising with cathepsin D in two morphologically distinct endocytic compartments. Similar results were obtained with mAb 3N7C2. (E,F) Lysosomes were pre-loaded with BSA-5 nm gold using a 4-hour pulse and a 20-hour chase to distinguish late endosomes and lysosomes. Nramp1 was clearly observed on the membranes of organelles with the morphology of late endosomes (E) and gold-loaded lysosomes (F). Bars, 200 nm.

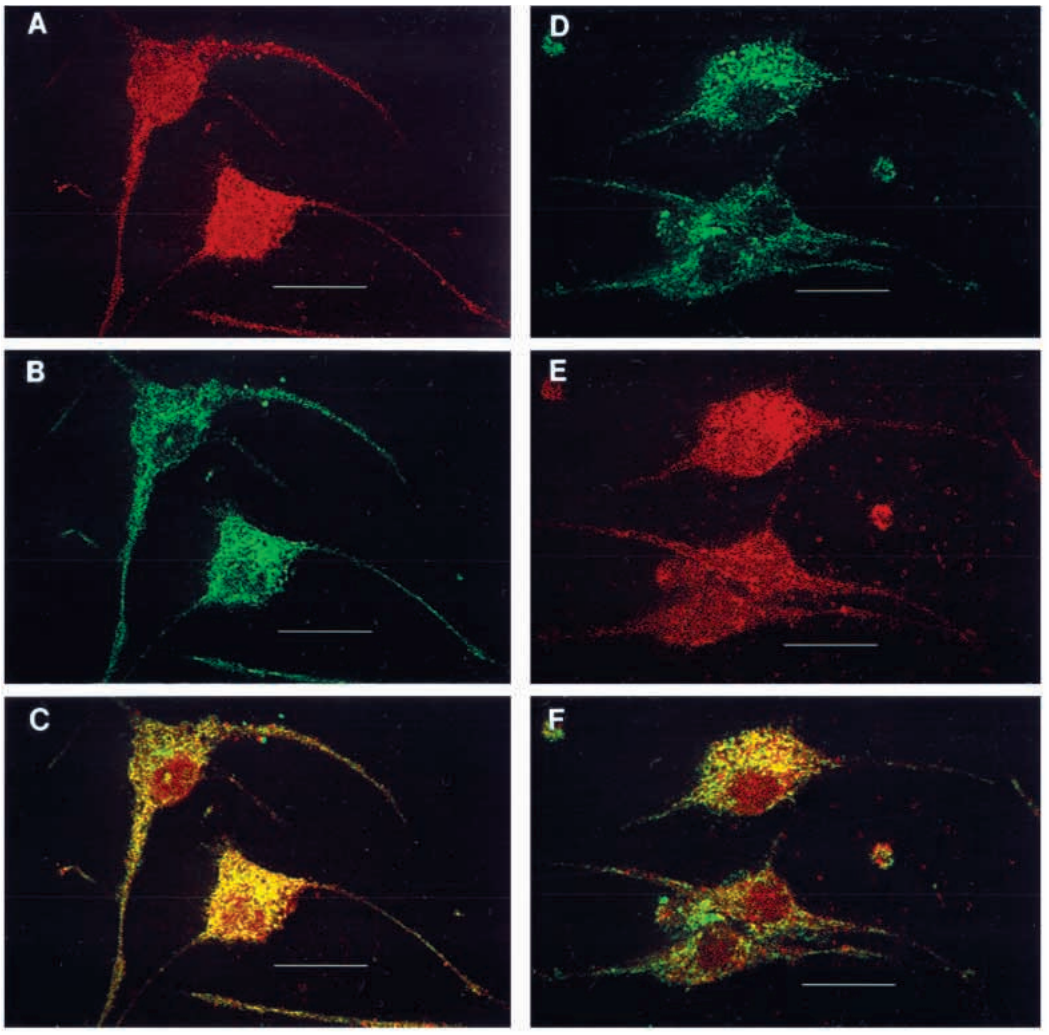

Fig. 5. Colocalistion of Nramp1 with cathepsin L and macrosialin in P388D1 macrophages activated for 24 hours with interferon-γ/LPS. Antibodies were visualised with secondary antibodies conjugated to Texas Red (A,E) or streptavidin-FITC (B,D). Nuclei were stained red with propidium iodide. (A) Texas Red immunolabelling of wild-type Nramp1 using mAb 2N7C3 distributed on vesicles throughout the cytoplasm; (B) parallel distribution of FITC green-labelled cathepsin L in the same cell; and (C) the merged image, with yellow identifying colocalisation of Nramp1 and cathepsin L. (D) FITC green-labelled wild-type Nramp1 stained with polyclonal anti-N-terminal Nramp1 distributed on vesicles throughout the cytoplasm; (E) parallel distribution of the Texas Red-labelled late endosomal marker macrosialin in the same cell; and (F) the merged image, with yellow identifying colocalisation of Nramp1 and macrosialin. Microscope settings: gain –1100; black level –2; iris 3.0 on both Texas Red and FITC channels. Bars, 25 μm.

an intracellular vesicular compartment (Atkinson et al., 1997), and colocalisation with markers of late endosomal and lysosomal compartments (Gruenheid et al., 1997). However, in constrast to the earlier report using confocal analysis alone (Gruenheid et al., 1997), our more accurate EM-gold colocalisation studies demonstrate that Nramp1 localises with Lamp1 and the cathepsins D and L in both electron-lucent late endosomal and electron-dense lysosomal compartments. Gruenheid et al. (1997) failed to see the colocalization with cathepsins D and L. Furthermore, our studies show that these electron-lucent and electron-dense compartments to which Nramp1 localises can be distinguished by colocalisation with antibodies to macrosialin on the former, and by colocalisation with pre-loaded BSA-5 nm gold in the latter. The colocalisations with cathepsin L and macrosialin were also readily observable at confocal microscope level. Hence, our results provide more accurate data on the localisation of Nramp1 using more sensitive methods.

One area in which our studies provide entirely new information on Nramp1 expression is in analysis of interferon-γ/LPS activated macrophages. This demonstrates a shift in the localisation pattern with activation. Quantitation by EM-gold shows a higher ratio of lysosomal:late endosomal labelling following activation, coincident with confocal visualisation of apparent dispersion of Nramp1-positive vesicles from a perinuclear location towards the periphery of the cell. The latter produced a striking confocal pattern of vesicles located along microtubular structures of the cell, consistent with previous studies showing microtubule associated protein-dependent binding of phagosomes to (Blocker et al., 1996), and bi-directional movement of phagosomes along (Blocker et al., 1997), microtubulues. This pattern of Nramp1 expression is compatible with the observation that NH_2-terminal domain of human NRAMP1 associates with alpha-and beta-tubulin of microtubules (Kishi et al., 1996), although we do not concurr with these workers that NRAMP1 localises to the plasma membrane. More likely would be the direct delivery of Nramp1 from the trans-Golgi network (TGN) to late endosomal/lysosomal compartments, which is also consistent with the presence of tyrosine-based endocytic targeting signals in the 5′ and 3′ ends of the molecule (Atkinson et al., 1997). Such signals have been implicated in directing the sorting of transmembrane proteins (Ohno et al., 1995; Marks et al., 1997), and can be read at more than one sorting site (Rohrer et al., 1996). In Nramp1, the C-terminal domain has a conserved Y residue in the context of a YGLP motif, and in the N-terminal domain in the context of YGSI and located within the putative SH3-binding domain (Barton et al., 1994). Both conform to the

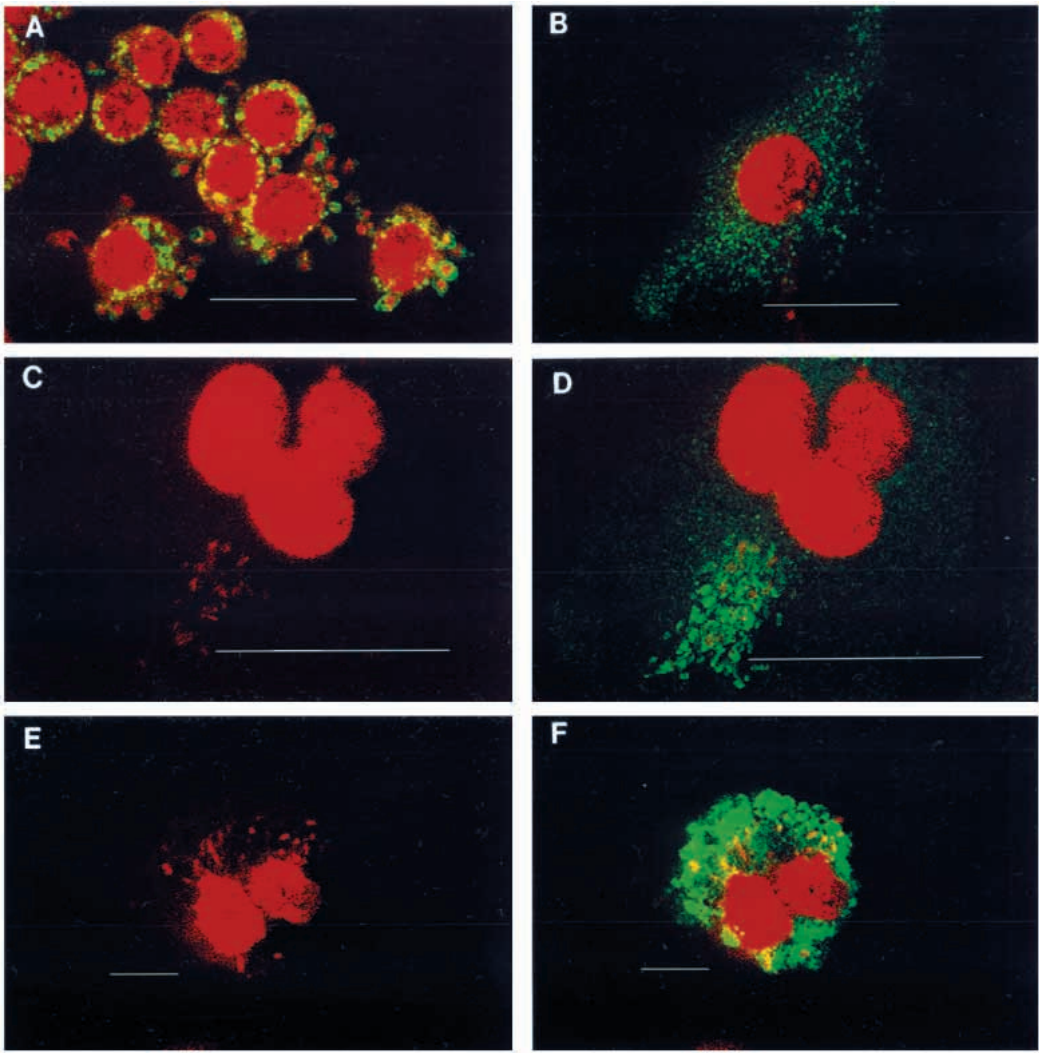

Fig. 6. Nramp1 localisation in Nramp1 mutant 2S stable transfectants infected for 24 hours with *L. major* LV39 metacyclics (A) and in activated (400 units/ml interferon-γ for 18 hours; 500 ng/ml LPS for 4 hours) Nramp1 wild-type (C,D) and mutant (E,F) bone marrow-derived macrophages infected for 2 hours with *M. avium.* Cells were labelled with polyclonal rabbit anti-C-terminal Nramp1, and counterstained with propridium iodide to detect host cell and pathogen nuclei. (A) Mutant Nramp1 in the membranes of *L. major*-containing phagosomes, which remain located in the perinuclear region. Similar results were obtained with Nramp1 mutant 10S and wild-type 7.5R transfectants. (B) Nramp1-positive vesicles dispersed throughout the cytoplasm of uninfected activated Nramp1 wild-type bone marrow-derived macrophages. (C) A cluster of *M. avium* within an infected cell; and (D) the merged image with wild-type Nramp1, demonstrating the migration of Nramp1-positive endocytic vesicles to *M. avium* phagosomes. (E) *M. avium* in the cytoplasm of an infected cell; and (F) the merged image with mutant Nramp1, demonstrating only partial migration of Nramp1-positive vesicles to *M. avium* phagosomes. Similar observations were made in resting macrophages and with mAbs. Microscope settings: gain −1500; black level −2; iris 2.0 (A,) 3.0 (B-F) green channel, 3.0 (A-F) red channel. Bars, 25 μm (A-D); 10 μm (E,F).

requirement for the Y residue to be present in a motif YXXZ, where X corresponds to any residue and Z to a hydrophobic residue (reviewed by Marks et al., 1997). For resident, integral membrane proteins of the endocytic pathway, these motifs have been defined within the cytoplasmic C-terminal domains. During phagocytosis, the delivery of new molecules to the maturing phagosome is less clear-cut, with opposing models suggesting that endosomal markers are acquired through multi-fusion events with endocytic compartments (Desjardins et al., 1994; Rohrer et al., 1996) or directly from the TGN prior to fusion with lysosomal compartments (Rohrer et al., 1996). In previous studies of Nramp1 delivery to latex bead phagosomes, Nramp1 was acquired by the phagosomal membrane with time kinetics similar to Lamp1, and clearly distinct from those of the early endosomal marker Rab5 (Gruenheid et al., 1997), suggesting a later fusion event. Whether Nramp1 N-terminal and C-terminal targeting sequences are performing different roles following activation and/or during phagocytosis is under investigation using mutagenised Nramp1 constructs in transfection studies.

Finally, our study here has provided the first direct visualisation of Nramp1 in relation to pathogen-containing phagosomes. It is well known that Nramp1 plays an essential role in host defence against intracellular pathogens. Infections under Nramp1 control enter the cell by receptor-mediated phagocytosis (*L. donovani* and *Mycobacterium* species) or macropinocytosis (*S. typhimurium*), both of which are driven by actin and result in the formation of phagosomes. As they mature, these phagosomes have been shown to acquire characteristics of late endosomes and lysosomes (de Chastellier et al., 1993; Lang et al., 1994; Sturgill-Koszycki et al., 1994, 1996; Rathman et al., 1996, 1997). However, the rate at which this occurs varies between micro-organisms and, for *M. avium* and *M. tuberculosis* in particular, phagosome maturation has been shown to be arrested in an early transitional stage, which acquires an immature form of cathepsin D from the TGN but remains accessible to internalized transferrin (Sturgill-Koszycki et al., 1996). Given this observation, and having established that Nramp1 localises to endocytic compartments involved in the formation of

phagolysosomes (Desjardins et al., 1994; Beron, 1995), we compared Nramp1 localisation following phagocytosis of *L. major* and *M. avium* in macrophages. In the case of *L. major*, clear fusion of Nramp1-positive vesicles with the pathogen-containing phagosome is consistent with previous studies demonstrating rapid fusion and survival of leishmanial parasites within mature phagolysosomes (Lang et al., 1994). Interestingly, these phagolysosomes retained the perinuclear location of late endosomes in the infected resting Nramp1-transfected RAW264.7 macrophages studied. This contrasted with dramatic migration of Nramp1-positive macrophages to the site of bacterial phagosomes in *M. avium*-infected bone marrow-derived macrophages, even without addition of the exogenous activating signals provided by interferon-γ/LPS. Although we have not yet accurately quantified the degree of convergence/fusion of Nramp1-positive vesicles and bacterial phagosomes, there was qualitative evidence that convergence was less efficient in macrophages carrying the Nramp1 mutant allele. This is consistent with previous studies demonstrating reduced rates of phagosome-lysosome fusion in Nramp1 mutant macrophages (de Chastellier et al., 1993). It is also of interest in relation to the earlier suggestion of arrested development of the *M. avium* phagosome (Sturgill-Koszycki et al., 1996), which was carried out using macrophages from Nramp1 mutant BALB/c mice. This arrested development may therefore be a feature of, or at least unnaturally prolonged in, Nramp1 mutant macrophages. There is also the possibility that Nramp1 may itself may be mechanistically involved in delivering intracellular signals for phagosome/endosome/lysosome fusions to occur. This clearly has important implications for any role Nramp1 might have in directly manipulating the micro-environment (and hence survival) of the pathogen. It will therefore be of importance to determine the precise kinetics of Nramp1 delivery to late endosomal/lysosomal compartments, and in particular to compare this to phagosomes formed after ingestion of pathogens (e.g. *Listeria monocytogenes*; Alvarez-Dominguez et al., 1996), which do or do not come under Nramp1 control. It will also be of interest to determine how this relates to any direct role which Nramp1 might have in regulating iron supply to the parasite, as opposed to the secondary role which regulation of cellular iron levels might have in controlling macrophage activation and antimicrobial activities.

We are indebted to Dr Paul Luzio, Department of Clinical Biochemistry, for providing access to the use of the confocal and electron microscopes, which were purchased from with funds provided by the British Medical Research Council. This work was supported by grants from The Wellcome Trust.

REFERENCES

Alvarez-Dominguez, C., Barbieri, A. M., Beron, W., Wandinger-Ness, A. and Stahl, P. D. (1996). Phagocytosed live *Listeria monocytogenes* influences Rab5 regulated *in vitro* phagosome-endosome fusion. *J. Biol. Chem.* **271,** 13834-13843.

Atkinson, P. G. P., Blackwell, J. M. and Barton, C. H. (1997). *Nramp1* locus encodes a 65 kDa interferon-gamma-inducible protein in murine macrophages. *Biochem J.* **325,** 779-786.

Atkinson, P. G. P. and Barton, C. H. (1998). Ectopic expression of Nramp1 in COS-1 cells modulates iron accumulation. *Eur. J. Biochem.* (in press).

Authier, F., Posner, B. I. and Bergeron, J. J. M. (1996). Minireview Endosomal proteolysis of internalized proteins. *FEBS Lett*. **389,** 55-60.

Barton, C. H., White, J. K., Roach, T. I. A. and Blackwell, J. M. (1994). NH_2-terminal sequence of macrophage-expressed natural resistance-associated macrophage protein (*Nramp*) encodes a proline/serine-rich putative *Src* homology 3-binding domain. *J. Exp. Med*. **179,** 1683-1687.

Barton, C. H., Whitehead, S. H. and Blackwell, J. M. (1995). *Nramp* transfection transfers *Ity/Lsh/Bcg*-related pleiotropic effects on macrophage activation: Influence on oxidative burst and nitric oxide pathways. *Mol. Med.* **1,** 267-279.

Beron, W., Alvarez-Dominguez, C., Mayorga, L. and Stahl, P. D. (1995). Membrane trafficking along the phagocytic pathway. *Trends Cell Biol*. **5,** 100-104.

Blackwell, J. M., Toole, S., King, M., Dawda, P., Roach, T. I. A. and Cooper, A. (1988). Analysis of *Lsh* gene expression in congenic B10.L-*Lsh*^{r} mice. *Curr. Top. Microbiol. Immunol*. **137,** 301-309.

Blackwell, J. M. (1989) (convenor). The macrophage resistance gene *Lsh/Ity/Bcg.* 27th Forum in Immunology. *Res. Immunol*. **140,** 767-828.

Blackwell, J. M. and Searle, S. (1998). Genetic regulation of macrophage activation: understanding the function of *Nramp1* (=*Ity/Lsh/Bcg*). *Immunol. Lett*., in press.

Blocker, A., Severin, F. F., Habermann, A., Hyman, A. A., Griffiths, G. and Burkhardt, J. K. (1996). Microtubule-associated protein-dependent binding of phagosomes to microtubules. *J. Biol. Chem*. **271,** 3803-3811.

Blocker, A., F. Severin, F., Burkhardt, J. K., Bingham, J. B., Yu, H., Olivo, J.-C., Schroer, T. A., Hyman, A. A. and Griffiths, G. (1997). Molecular requirements for bi-directional movement of phagosomes along microtubules. *J. Cell Biol*. **137,** 113-129.

Bright, N. A., Reaves, B. J., Mullock, B. M., and Luzio, J. P. (1997). Dense core lysosomes can fuse with late endosomes and are re-formed from the resultant hybrid organelles. *J. Cell Sci.* **110,** 2027-2040.

Brown, D. H., Lafuse, W. P. and Zwilling B. S. (1997). Stabilized expression of mRNA is associated with mycobacterial resistance controlled by Nramp1. *Infect. Immun*. **65,** 597-603.

Cellier, M., Prive, G., Belouchi, A., Kwan, T., Rodrigues, V., Chia, W. and Gros, P. (1995). Nramp defines a family of membrane proteins. *Proc. Nat. Acad. Sci. USA* **92,** 10089-10093.

Cellier, M., Belouchi, A. and Gros, P. (1996). Resistance to intracellular infections: Comparative genomic analysis of *Nramp1*. *Trends Genet.* **12,** 201-204.

Clark, M. and Waldmann, H. (1986). Production of murine monoclonal antibodies. In *Methods in Haematology: Monoclonal Antibodies* (ed. P. C. L. Beverley), pp. 1-20. Churchill Livingstone London.

Cooper, A., Rosen, H. and Blackwell, J. M. (1988). Monoclonal antibodies that recognise different epitopes of the macrophage type three complement receptor differ in their ability to inhibit binding of *Leishmania* promastigotes harvested at different phases of their growth cycle. *Immunology* **65,** 511-514.

Dawe, C. J. and Potter, M. (1957). Morphologic and biologic progression of a lymphoid neoplasm of the mouse *in vivo* and *in vitro*. *Am. J. Pathol*. **33,** 603.

de Chastellier, C., Frehel, C., Offredo, C. and Skamene, E. (1993). Implication of the phagosome-lysosome fusion in restriction of *Mycobacterium avium* growth in bone marrow macrophages from genetically resistant mice. *Infect. Immun*. **61,** 3775-3784.

Desjardins, M., Huber, L. A., Parton, R. G. and Griffiths, G. (1994). Biogenesis of phagolysosomes proceeds through a sequential series of interactions with the endocytic apparatus. *J. Cell Biol*. **124,** 677-688.

Diment, S., Leech, M. S. and Stahl, P. D. (1988). Cathepsin D is membrane-associated in macrophage endosomes. *J. Biol. Chem*. **263,** 6901-6907.

Geuze, H. J., Slot, J. W., Strous, G. J., Hasilik, A. and von Figura, K. (1985). Possible pathways for lysosomal enzyme delivery. *J. Cell Biol*. **101,** 2253-2262.

Geuze, H. J., Stoorvogel, W., Strous, G. J., Slot, J. W., Bleekemolen, J. E. and Mellman, I. (1988). Sorting of mannose 6-phosphate receptors and lysosomal membrane proteins in endocytic vesicles. *J. Cell Biol*. **107,** 2491-2501.

Govoni, G., Vidal, S., Cellier, M., Lepage, P., Malo, D. and Gros, P. (1995). Genomic structure, promoter sequence, and induction of expression of the mouse *Nramp1* gene in macrophages. *Genomics* **27,** 9-19.

Griffiths, G. (1993). *Fine Structure Immunocytochemistry*, pp. 1-459. Springer-Verlag, Berlin.

Griffiths, G., Hoflack, B., Simons, K., Mellman, I. and Kornfeld, S. (1988). The mannose 6-phosphate receptor and the biogenesis of lysosomes. *Cell* **52,** 329-341.

Gruenheid, S., Pinner, E., Desjardins, M. and Gros, P. (1997). Natural

resistance to infection with intracellular pathogens: The *Nramp1* protein is recruited to the membrane of the phagosome. *J. Exp. Med.* **185,** 717-730.

Gunshin, H., Mackenzie, B., Berger, U. V., Gunshin, Y., Romero, M. F., Boron, W. F., Nussberger, S., Gollan, J. L. and Hediger, M. A. (1997). Cloning and characterization of a mammalian proton-coupled metal- ion transporter. *Nature* **388,** 482-488.

High, S. and Laird, V. (1997). Membrane protein biosynthesis-all sewn up? *Trends Cell Biol*. **7,** 206-210.

Kishi, F., Yoshida, T. and Aiso, S. (1996). Location of NRAMP1 molecule on the plasma membrane and its association with microtubules. *Mol. Immunol.* **33**, 1241-1246.

Lah, T. T., Hawley, M., Rock, K. L. and Goldberg, A. L. (1995). Gamma-interferon causes a selective induction of the lysosomal proteases, cathepsins B and L, in macrophages. *FEBS Lett.* **363,** 86-89.

Lang, L., Hellio, R., Kaye, P. M. and Antoine, J.-C. (1994). *Leishmania donovani*-infected macrophages: characterization of the parasitophorous vacuole and potential role of this organelle in antigen presentation. *J. Cell Sci.* **107,** 2137-2150.

Ludwig, T., Griffiths, G. and Hoflack, B. (1991). Distribution of newly synthesized lysosomal enzymes in the endocytic pathway of normal rat kidney cells. *J. Cell Biol*. **115,** 1561-1572.

Marks, M. S., Ohno, H., Kirchhausen, T. and Bonifacino, J. S. (1997). Protein sorting by tyrosine-based signals: adapting to the Ys and wherefores. *Trends Cell Biol*. **7,** 124-128.

Mellman, I. (1996). Endocytosis and molecular sorting. *Ann. Rev. Cell Dev. Biol*. **12,** 575-625.

Ohno, H., Stewart, J., Fournier, M-C., Bosshart, H., Rhee, I., Miyatake, S., Saito, T., Gallusser, A., Kirchhausen, T. and Bonifacino. J. S. (1995). Interaction of tyrosine-based sorting signals with clathrin-associated proteins. *Science* **269,** 1872-1875.

Rabinowitz, S., Horstmann, H., Gordon, S. and Griffiths, G. (1992). Immunocytochemical characterization of the endocytic and phagolysosomal compartments in peritoneal macrophages. *J. Cell Biol.* **116,** 95-112.

Raschke, W. C., Baird, S., Ralph, R. and Nakoinz, I. (1978). Functional macrophage cell lines transformed by Abelson leukemia virus. *Cell*. **15,** 261-267.

Rathman, M., Sjaastad, M. D. and Falkow, S. (1996). Acidification of phagosomes containing *Salmonella typhimurium* in murine macrophages. *Infect. Immun.* **64,** 2765-2773.

Rathman, M., Barker, L. P. and Falkow, S. (1997). The unique trafficking pattern of *Salmonella typhimurium*-containing phagosomes in murine macrophages is independent of the mechanism of bacterial entry. *Infect. Immun*. **65,** 1475-1485.

Roach, T. I. A., Barton, C. H., Chatterjee, D. and Blackwell, J. M. (1993). Macrophage activation: lipoarabinomannan (LAM) from avirulent and virulent strains of *Mycobacterium tuberculosis* differentially induces the early genes c-fos, KC, JE and TNF-alpha. *J. Immunol.* **150,** 1886-1896.

Rohrer, J., Schweizer, A., Russell, D. and Kornfeld, S. (1996). The targeting of Lamp1 to lysosomes is dependent on the spacing of its cytoplasmic tail tyrosine sorting motif relative to the membrane. *J. Cell Biol*. **132,** 565-576.

Schaible, U. E., Sturgill-Koszycki, S., Schlesinger, P. H. and Russell, D. G. (1998). Cytokine activation leads to acidification and increases maturation of *Mycobacterium avium*-containing phagosomes in murine macrophages. *J. Immunol.* **160,** 1290-1296.

Schurr, E., Malo, D., Radzioch, D., Buschman, E., Morgan, K., Gros, P., and Skamene, E. (1991). Genetic control of innate resistance to mycobacterial infections. *Immunol. Today*. **12,** A42-A45.

Slootstra, J. W., Puijk, W. C., Ligtvoet, G. J., Langeveld, J. P. M. and Meloen, R. H. (1996). Structural aspects of antibody-antigen interaction revealed through small random peptide libraries. *Mol. Div*. **1,** 87-96.

Slot, J. W. and Geuze, H. J. (1983). The use of protein A-colloidal gold (PAG) complexes as immunolabels in ultrathin frozen sections. In *Immunocytochemistry* (ed. A. C. Cuello), pp. 323-346. John Wiley and Sons, Chichester.

Slot, J. W. and Geuze, H. J. (1985). A new method of preparing gold probes for multiple-labeling cytochemistry. *Eur. J. Cell Biol.* **38,** 87-93.

Slot, J. W., Geuze, H. J., Gigengack, S., Lienhard, G. E. and James, D. E. (1991). Immuno-localization of the insulin regulatable glucose transporter in brown adipose tissue of the rat. *J. Cell Biol*. **113,** 123-135.

Smith, D. B. and Johnson, K. S. (1988). Single step purification of polypeptides expressed in *Escherichia coli* as fusions with glutathione S-transferase. *Gene* **67,** 31-40.

Smith, M. J. and Koch, G. L. E. (1987). Differential expression of murine macrophage surface glycoprotein antigens in intracellular membranes. *J. Cell. Sci*. **87,** 113-119.

Sturgill-Koszycki, S., Schlesinger, P., Chakraborty, P., Haddix, P. L., Collins, H. L., Fok, A. K., Allen, R. D., Gluck, S. L., Heuser, J. and Russell, D. G. (1994). Lack of the acidification of the *Mycobacterium* phagosomes produced by exclusion of the vesicle proton-ATPase. *Science* **263,** 678-681.

Sturgill-Koszycki, S., Schaible, U. E. and Russell, D. G. (1996). *Mycobacterium*-containing phagosomes are accessible to early endosomes and reflect a transitional state in the normal phagosome biogenesis. *EMBO J.* **15,** 6960-6968.

Supek, F., Supekova, L., Nelson, H. and Nelson, N. (1996). A yeast manganese transporter related to the macrophage protein involved in conferring resistance to mycobacteria. *Proc. Nat. Acad. Sci. USA* **93,** 5105-5110.

Tokuyasu, K. T. (1978). A study of positive staining of ultrathin frozen sections. *J. Ultrastructure Res.* **63,** 287-307.

Vidal, S. M., Malo, D., Vogan, K., Skamene, E. and Gros, P. (1993). Natural resistance to infection with intracellular paraistes: isolation of a candidate for *Bcg. Cell* **73,** 469-485.

Vidal, S., Tremblay, M. L., Govoni, G., Gauthier, S., Sebastiani, G., Malo, D., Skamene, E., Olivier, M., Jothy, S. and Gros, P. (1995). The *Ity/Lsh/Bcg* locus: natural resistance to infection with intracellular parasites is abrogated by disruption of the *Nramp1* gene. *J. Exp. Med*. **182,** 655-666.

Vidal, S. M., Pinner, E., Lepage, P., Gauthier, S. and Gros, P. (1996). Natural resistance to intracellular infections. *J. Immunol*. **157,** 3559-3568.

von Figura, K. and Hasilik, A. (1986). Lysosomal enzymes and their receptors. *Ann. Rev. Biochem*. **55,** 167-193.

Wiederanders, B. and Kirschke, H. (1986). Antibodies to rat liver cathepsins; characterization and use for the identification of enzyme precursors. *Biomed. Biochim. Acta* **45,** 1421-1431.